



LAWRENCE
LIVERMORE
NATIONAL
LABORATORY

Understanding the creation of & reducing surface microroughness during polishing & post-processing of glass optics

T. Suratwala

September 22, 2016

Disclaimer

This document was prepared as an account of work sponsored by an agency of the United States government. Neither the United States government nor Lawrence Livermore National Security, LLC, nor any of their employees makes any warranty, expressed or implied, or assumes any legal liability or responsibility for the accuracy, completeness, or usefulness of any information, apparatus, product, or process disclosed, or represents that its use would not infringe privately owned rights. Reference herein to any specific commercial product, process, or service by trade name, trademark, manufacturer, or otherwise does not necessarily constitute or imply its endorsement, recommendation, or favoring by the United States government or Lawrence Livermore National Security, LLC. The views and opinions of authors expressed herein do not necessarily state or reflect those of the United States government or Lawrence Livermore National Security, LLC, and shall not be used for advertising or product endorsement purposes.

This work performed under the auspices of the U.S. Department of Energy by Lawrence Livermore National Laboratory under Contract DE-AC52-07NA27344.

LDRD FINAL REPORT

Understanding the creation of & reducing surface microroughness during polishing & post-processing of glass optics

Tayyab Suratwala (14-ERD-042)

Abstract

In the follow study, we have developed a detailed understanding of the chemical and mechanical microscopic interactions that occur during polishing affecting the resulting surface microroughness of the workpiece. Through targeted experiments and modeling, the quantitative relationships of many important polishing parameters & characteristics affecting surface microroughness have been determined. These behaviors and phenomena have been described by a number of models including: (a) the Ensemble Hertzian Multi Gap (EHMG) model used to predict the removal rate and roughness at atomic force microscope (AFM) scale lengths as a function of various polishing parameters, (b) the Island Distribution Gap (IDG) model used to predict the roughness at larger scale lengths, (c) the Deraguin-Verwey-Landau-Overbeek (DLVO) 3-body electrostatic colloidal model used to predict the interaction of slurry particles at the interface and roughness behavior as a function of pH, and (d) a diffusion/chemical reaction rate model of the incorporation of impurities species into the polishing surface layer (called the Bielby layer). Based on this improved understanding, novel strategies to polish the workpiece have been developed simultaneously leading to both ultrasoft surfaces and high material removal rates. Some of these strategies include: (a) use of narrow PSD slurries, (b) a novel diamond conditioning recipe of the lap to increase the active contact area between the workpiece and lap without destroying its surface figure, (c) proper control of pH for a given glass type to allow for a uniform distribution of slurry particles at the interface, and (d) increase in applied load just up to the transition between molecular to plastic removal regime for a single slurry particle. These techniques have been incorporated into a previously developed finishing process called Convergent Polishing leading to not just economical finishing process with improved surface figure control, but also simultaneously leading to low roughness surface with high removal rates.

Background and Research Objectives

In the past decade, there have been significant advancement in optical finishing science including improving the macroscopic aspects (e.g., overall surface figure) and reducing isolated imperfections (e.g., scratches). At the start of this study (FY14), much less was understood regarding the microscopic scale length interactions that occur during polishing, specifically those influencing the microroughness and power spectra of the surface. The ability to fabricate very low roughness (2-4 Angstrom rms) surfaces has been around since the 80's; however, these polishing techniques have been derived from an artisan approach and the processes are very time consuming and expensive. Low roughness and low power spectra surfaces are highly desired for high-end x-ray optics, high fluence laser optics (such as for the National Ignition Facility (NIF)), and telescope

optics to minimize optical scatter and reduce laser beam contrast.

The basic objectives of the proposed study have been achieved as originally proposed; They are: 1) to gain a scientific understanding of the microscopic and chemical interactions that occur during polishing and how they influence the microroughness of glass surfaces; 2) to develop novel, cost effective methods to achieve very low roughness on optical glass surfaces both after polishing & post-processing.

Scientific Approach and Accomplishments

Our approach is to investigate a number of proposed parameters that can occur at the polishing interface that likely affect the workpiece roughness (see Figure 1). Each of these was investigated in detail. These interactions were grouped into 4 major areas which are described below.

1) Beilby Layer Studies: During polishing, the final surface of the workpiece consists of an outer surface layer (10's of nm) that has been modified both chemically and mechanically. Historically, this surface layer has been referred to as the Beilby layer. The mechanism for its creation has been largely debated on whether it is a redeposition or as a result of diffusion plus reaction effects. In this part of this study, the chemical characteristics and the proposed formation mechanisms of the Beilby layer on polished fused silica glasses were determined. Fused silica glass samples were polished using different slurries, polyurethane pads, and at different rotation rates. The concentration profiles of several key contaminants, such as Ce, K and H, were measured in the near surface layer of the polished samples using Secondary Ion Mass Spectroscopy. The penetration of K, originating from KOH used for pH control during polishing, *decreased* with increase in polishing material removal rate. In contrast, penetration of the Ce and H *increased* with increase in polishing removal rate. The resulting K concentration depth profiles are described using a two-step diffusion process: (1) steady-state moving boundary diffusion (due to material removal during polishing) followed by (2) simple diffusion during ambient post-polishing storage. On the other hand, the observed Ce profiles are inconsistent with diffusion based transport. Rather we proposed that Ce penetration is governed by the ratio of Ce-O-Si and Si-O-Si hydrolysis rates; where this ratio increases with interface temperature (which increases with polishing material removal rate) resulting in greater Ce penetration into the Beilby layer. These new insights into the chemistry of the Beilby layer, combined together with details of the single particle removal function during polishing, are used to develop a more detailed and quantitative picture of the polishing process, and the formation of the Beilby layer and surface roughness (see Figure 2) [1].

2) Removal Function Studies: In this part of the study, the nano-mechanical deformations on glass surfaces near the elastic-plastic load boundary have been measured on various glasses by nanoscratching using an AFM to mimic the mechanical interactions of polishing particles during optical polishing [3]. Nanoscratches were created in air and aqueous environments using a 150 nm radius diamond coated tip on polished fused silica, borosilicate, and phosphate glass surfaces; the topology of the nanoscratches were then

characterized by AFM. Using load ranges expected on slurry particles during glass polishing (0.05-200 μN), plastic type scratches were observed with depths in the nm range. Nanoscratching in air generally showed deeper & narrower scratches with more pileup compared to nanoscratching in water, especially on fused silica glass. For phosphate glass, the load dependence of the removal depth was consistent with that expected from Hertzian mechanics. However, for fused silica and borosilicate glass in this load range, the deformation depth showed a weak dependence with load. In water, the removal depths were determined as 0.3-0.55 nm/pass for fused silica, 0.85 nm/pass for borosilicate glass, and 2.4 nm/pass for phosphate glass. The combined nanoscratching results were utilized to define the composite removal function (i.e., removal depth) for a single polishing particle as a function of load, spanning the chemical to the plastic removal regimes (Figure 3). This removal function serves as an important set of parameters used in the EHMGM model to predict the roughness of polished workpiece.

3) Polishing Studies on Roughness: EHMGM Model [2,4]. Here, a comprehensive set of glass samples (fused silica, phosphate, and borosilicate) were polished using various slurry PSDs, slurry concentrations, and pad treatments; workpiece roughness and removal rate were subsequently measured. Using an expanded Hertzian contact model, called the Ensemble Hertzian Multi-gap (EHMGM) model, a platform has been developed to understand the microscopic interface interactions and to predict trends of the removal rate and surface roughness for a variety of polishing parameters. The EHMGM model is based on multiple Hertzian contacts of slurry particles at the workpiece-pad interface in which the pad deflection and the effective interface gap at each pad asperity height are determined. Using this, the interface contact area and each particle's penetration, load, and contact zone are determined which are used to calculate the material removal rate and simulate the surface roughness. Each of the key polishing variables investigated is shown to affect the material removal rate, whose changes are dominated by very different microscopic interactions. Slurry PSD impacts the load per particle distribution and the fraction of particles removing material by plastic removal. The slurry concentration impacts the areal number density of particles and fraction of load on particles versus pad. The pad topography impacts the fraction of pad area making contact with the workpiece. The glass composition predominantly impacts the depth of plastic removal. Also, the results show that the dominant factor controlling surface roughness is the slurry PSD followed by the glass material's removal function and the pad topography. The model compares well with the experimental data over a variety of polishing conditions for both removal rate and roughness (see for example Figure 4). Also, the model can be extended to provide insights and strategies to develop practical, economic processes for obtaining ultra-low roughness surfaces while simultaneously maintaining high material removal rates.

IDGM Model [5]. In this part of this study, the polishing slurry pH and the generation glass removal products are shown to influence the slurry particle spatial and height distribution at the polishing interface and the resulting roughness of the glass workpiece. The AFM roughness was largely invariant with pH, suggesting the removal function of a single particle is unchanged with pH. However, the μ -roughness changed significantly, increasing linearly with pH for phosphate glass and having a maximum at an intermediate

pH for fused silica. In addition, the spatial and height distribution of slurry particles on the pad (as measured by laser confocal microscopy) was determined to be distinctly different at low and high pH during phosphate glass polishing. The zeta potential as a function of pH was measured for the workpiece, slurry and pad with and without surrogate glass products (K_3PO_4 for phosphate glass and $Si(OH)_4$ for silica). The addition of K_3PO_4 significantly raised the zeta potential, while addition of $Si(OH)_4$ had little effect on the zeta potential. An electrostatic DLVO 3-body force model, using the measured zeta potentials, was used to calculate the particle-particle, particle-workpiece, and particle-pad attractive & repulsive forces as a function of pH and the incorporation of glass products at the interface. The model predicted an increase in particle-pad attraction with increase in pH and phosphate glass products consistent with the measured slurry distribution on the pads during phosphate glass polishing. Finally, a slurry 'island' distribution gap (IDG) model has been formulated which utilizes the measured interface slurry distributions and a load balance to determine the interface gap, the contact area fraction, and the load on each slurry 'island'. The IDG model was then used to simulate the workpiece surface topography and μ -roughness; the results show an increase in roughness with pH similar to that observed experimentally.

4) Roughness & Redeposition: For the final major task, the focus was to determine the propensity of slurry particles to deposit on the workpiece surface as function of slurry chemical properties and workpiece roughness. Particle adsorption was explored in a model polishing system, consisting of silica colloids and like-charged silica surfaces [6]. The adsorption was monitored in situ under various suspension conditions, in the absence of surfactants or organic modifiers, using a quartz crystal microbalance with dissipation monitoring (QCM-D). Adsorption changes with particle concentration, particle size, pH, ionic strength and ionic composition were quantified by QCM-D and further characterized ex situ by atomic force microscopy. Transitions from near-zero adsorption to measurable adsorption were compared with predictions made using the DLVO theory. In addition, the impact of silica surface roughness on the propensity for particle adsorption was studied on various length scales by intentionally roughening the QCM sensor surface. It was found that a change in silica surface roughness from 1.2 nm (rms) to 2.7 nm (rms) resulted in an increase in silica particle adsorption of 5-fold for 50-nm diameter particles and 1.5-fold for 100-nm diameter particles—far exceeding coverage levels achievable by altering solution conditions alone. These sets of electrostatic interactions provide insight to the adhesion of particles both during polishing and during post-cleaning processes.

Impact on Mission

The scientific understanding developed from this study paves the way to the development of improved, low cost finishing processes. The process strategies developed are being technology transferred to processes for making high value, fusion laser optics with lower roughness (leading to lower scatter & laser beam contrast). For example, these strategies have been incorporated into a previously developed finishing process called Convergent Polishing (leading to not just economical finishing process with improved surface figure control but also simultaneously leading to low roughness surface with high removal rates)

which is currently at the pilot production stage for fabricating NIF optics. Additionally, this study has resulted in a series of peer reviewed journal publications which have been of high interest to those in the fields of optical fabrication, chemical-mechanical polishing, and laser science (see references).

Conclusion

We have developed a detailed understanding of the chemical and mechanical microscopic interactions that occur during polishing affecting the resulting surface microroughness of the workpiece. As a result, novel strategies to polish the workpiece have been developed simultaneously leading to both ultrasoft surfaces and high material removal rates. For example, these strategies have been incorporated into a previously developed finishing process called Convergent Polishing, which is in the pilot stage of finishing optics for the NIF. The Convergent Polishing technology is then targeted to be technology transferred to private industry, specifically optical fabricators of NIF optics.

References

1. T. Suratwala, R. Steele, L. Wong, M. Feit, P. Miller, R. Dylla-Spears, N. Shen, R. Desjardin, "Chemistry & formation of the Bielby layer during polishing of fused silica glass surfaces" *J. Am. Ceram. Soc.* **98**(8) 2395–2402 (2015).
2. T. Suratwala, R. Steele, M. Feit, N. Shen, R. Dylla-Spears, L. Wong, P. Miller, R. Desjardin, S. Elhadj, "Mechanism & simulation of removal rate & surface roughness during optical polishing of glasses" *J. Am. Ceram. Soc.* **99**(6) 1974–1984 (2016).
3. N. Shen, T. Suratwala, W. Steele, L. Wong, M. Feit, P. Miller, R. Dylla-Spears, R. Desjardin, "Nanoscratching of Optical Glass Surfaces Near the Elastic–Plastic Load Boundary to Mimic the Mechanics of Polishing Particles" *J. Am. Ceram. Soc.* **99**(5) 1477–1484 (2016).
4. T. Suratwala, M. Feit, R. Steele, L. Wong, N. Shen, R. Dylla-Spears, R. Desjardin, D. Mason, P. Geraghty, P. Miller, S. Baxamusa "Microscopic removal function & the relationship between slurry particle size distribution & workpiece roughness during pad polishing" *J. Am. Ceram. Soc.* **97**(1) 81–91 (2014).
5. T. Suratwala, R. Steele, M. Feit, N. Shen, L. Wong, R. Dylla-Spears, R. Desjardin, S. Elhadj, P. Miller, "Relationship between surface μ -roughness & interface slurry particle spatial distribution during glass polishing" to be submitted to *J. Am. Ceram. Soc.*(2016).
6. R. Dylla-Spears, L. Wong, N. Shen, R. Steele, T. Lee, J. Menapace, P. Miller, M. Feit, and T. Suratwala, "Adsorption of silica colloids onto like-charged silica surfaces of different roughness" to be submitted to *Colloids and Surfaces A: Physicochemical and Engineering Aspects* (2016).

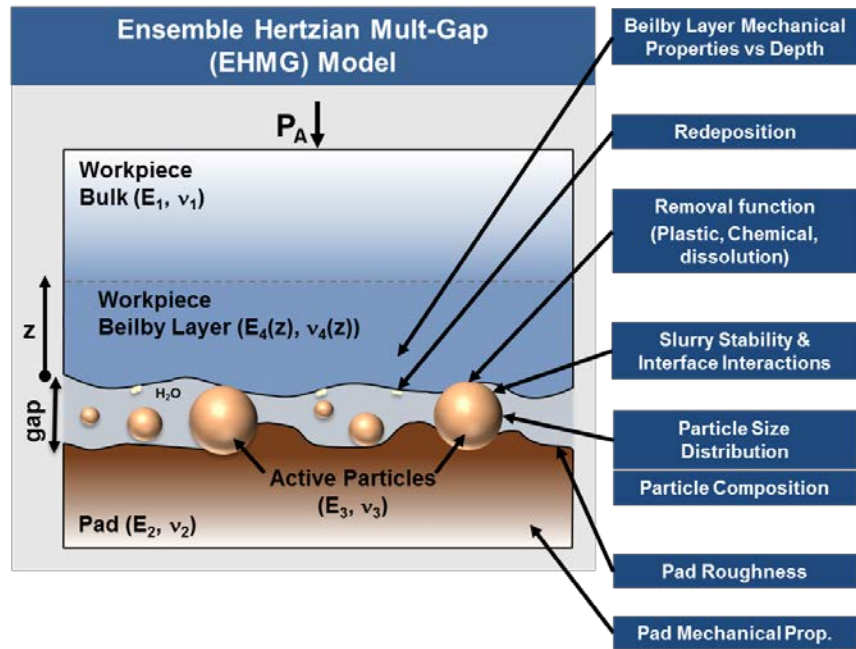


Figure 1: Schematic illustrating parameters affecting material removal and resulting surface roughness during polishing that have been investigated in this study.

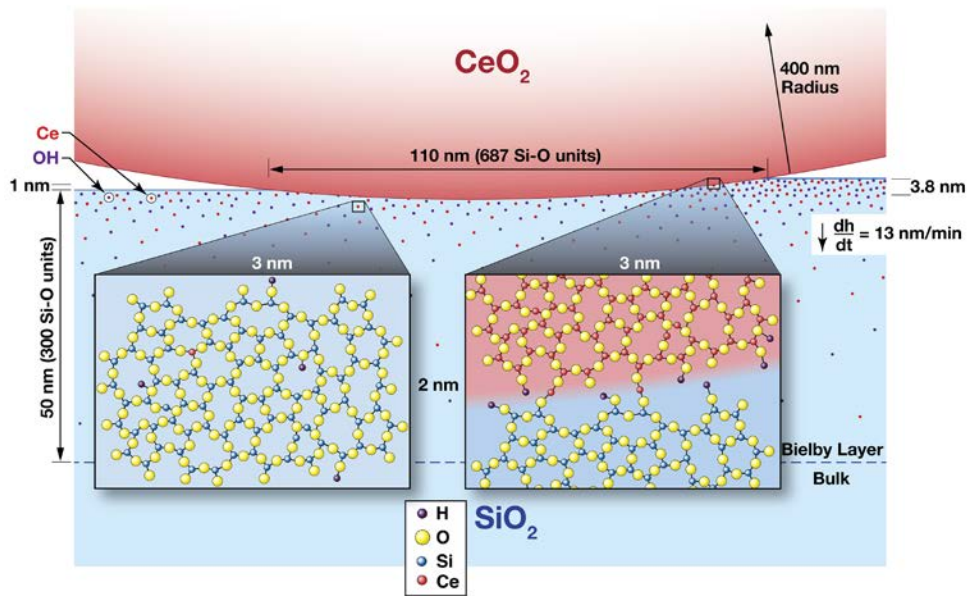


Figure 2: Schematic representation of proposed chemical and structural model of the polishing process and the Beilby layer [1].

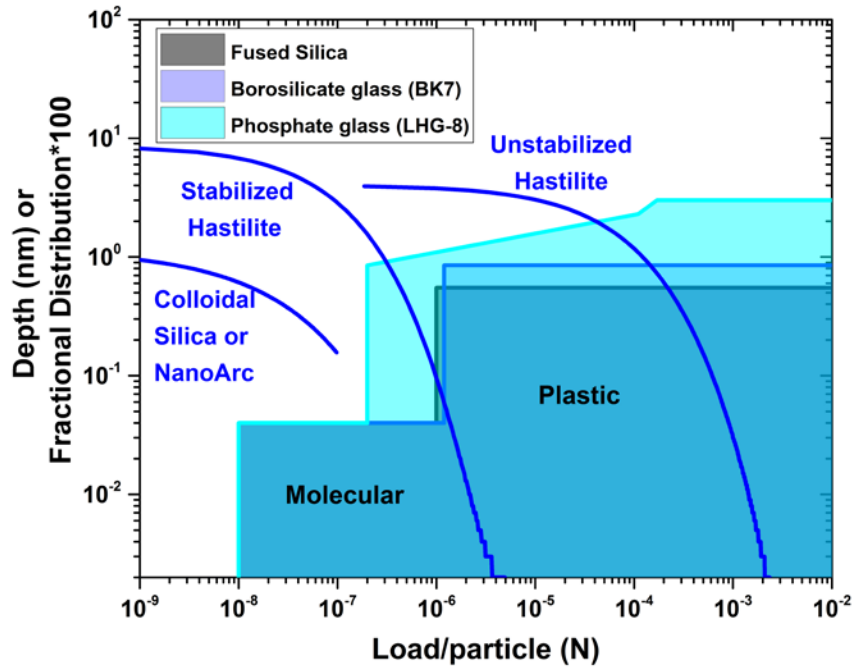


Figure 3. Measured removal function (shaded regions) as a function of load for individual slurry particles; and calculated load per particle distribution (lines) for three selected slurries using the EHMGM model [2,3].

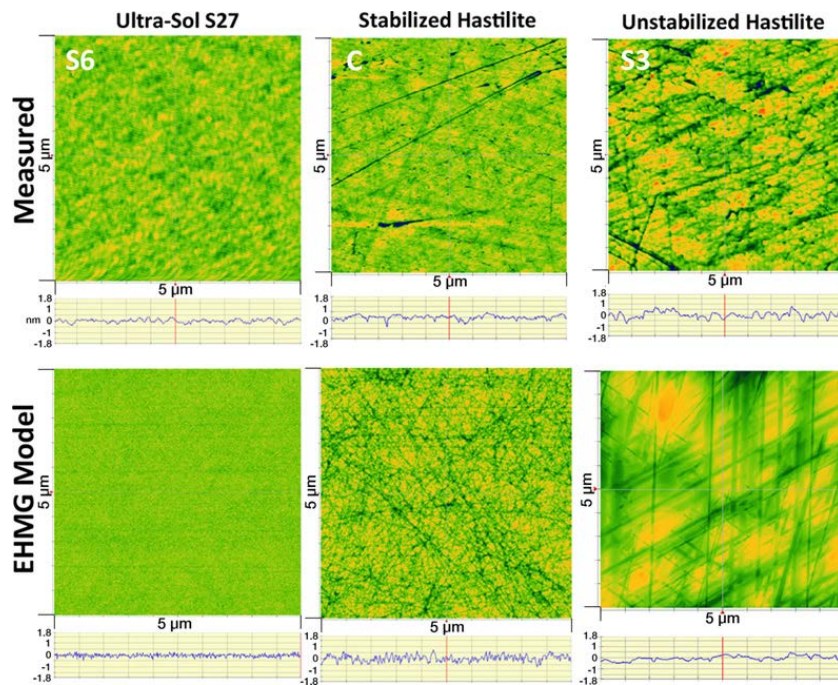


Figure 4: Comparison of measured AFM roughness ($5 \mu\text{m} \times 5 \mu\text{m}$) with that simulated with the EHMGM model for selected samples in the (a) slurry PSD series, (b) pad topography series, and (c) glass type series [2].